2019 IEEE/RSJ International Conference on Intelligent Robots and Systems (IROS)
Macau, China, November 4-8, 2019

# Robust Deformation Model Approximation for Robotic Cable Manipulation

Shiyu Jin*, Changhao Wang* and Masayoshi Tomizuka

***Abstract*— Cable manipulation is a challenging task for robots. The major challenge is that cables have high degrees of freedom and are easy to deform during manipulation. In this paper, we propose a novel framework SPR-RWLS to manipulate cables, which includes real-time cable tracking and robust local deformation model approximation. For cable tracking, structure preserved registration (SPR) is utilized to robustly estimate the movement of selected points on a cable even in the presence of sensor noise, outliers, and occlusions. Robust weighted least squares (RWLS) is then applied to calculate the local deformation model of the cable under uncertainties. We show that SPR-RWLS enables the dual-arm robots to manipulate cables with different thicknesses and lengths to different desired curvatures in multiple scenarios. We also show that real-time implementation of the proposed method can be simplified by parallel computation.**

## I. Introduction

Robotic cable manipulation has a wide range of applications, such as cable harnessing in factories, thread packing in production lines and suturing in medical surgeries. However, these tasks are challenging for robots. Compared with rigid objects, models of cables are high dimensional and computationally expensive. Besides, such an object can easily deform to unexpected shapes during manipulation, which may make the manipulation process fail.

There are already some studies on robotic cable manipulation. Many of them are model-based methods. The deformation properties of the cable in terms of stiffness, Young's modules, and/or FEM coefficients are required to build models for trajectory planning. However, such deformation parameters are difficult to estimate accurately and may even change during the manipulation process, especially for objects made by nonlinear elastic or plastic materials.

In this paper, we introduce a robust online deformation model approximation method for cable manipulation planning. A deformation model is constructed to describe the relation between the movement of the robots end-effectors and the displacement of the cable. The idea of the online deformation model approximation was first proposed by Navarro-Alarcon [6]. Cables have infinite degrees of freedom and it is hard to find an explicit model. Instead of finding a global model, real-time data is utilized for local linear model approximation. After the model is obtained, we find the pseudo-inverse of the model, which takes the desired movement of the cable as the input and the velocity of the robots end-effectors as the output. As the robots manipulate the cable, the deformation model is updated online using the real-time data.

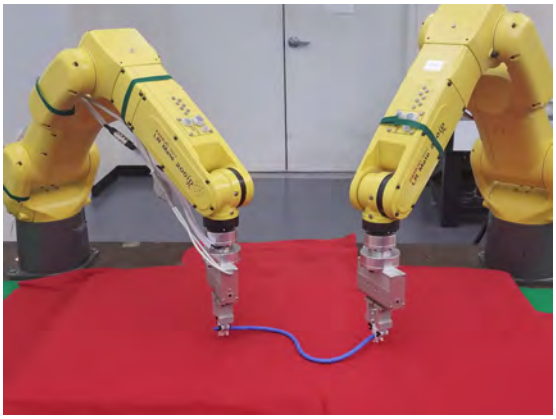

Fig. 1. Two robots manipulating a cable to a desired shape

In order to approximate the local deformation model of the cable, the motion data of the robots end-effectors and the cable are required. The motion of the end-effectors can be accurately obtained by solving forward kinematics. However, the motion of the cable is hard to obtain without the help of markers. Sensor noise and occlusions could introduce uncertainties when estimating the motion of the cable. Such uncertainties significantly affect the accuracy of the approximate deformation model.

To handle the above challenges, we propose a framework that is robust in both cable tracking and model approximation. For cable tracking, the core technique we use is called structure preserved registration (SPR) [2], which is a robust non-rigid registration method for mapping one point set to another. Considering both global and local structure, SPR can robustly estimate the motion of the deformable object in real-time even in the presence of sensor noise, outliers, and occlusions. For model approximation, we take tracking uncertainties into account by solving a robust optimization problem. We formulate the problem as a 'Min-Max' problem, where the maximization takes the worst case of the measurement uncertainty into account, and the minimization penalizes the cost function to find an optimal deformation model. The deformation model is then utilized to plan a trajectory to manipulate the cable.

The remainder of this paper is organized as follows. Section II introduces related works on the cable tracking and manipulation. Section III describes the SPR method for cable representation and tracking. Section IV explains the local model approximation method using robust optimization. Sec-

*: Both authors contributed equally to this work.
Department of Mechanical Engineering, University of California, Berkeley, CA, USA. {jsy, changhaowang, tomizuka}@berkeley.edu

tion V explains the design of the framework, which includes point tracking, local model approximation and trajectory planning modules. Section VI tests the performance of the proposed method by a series of experiments. Supplementary videos can be found in [17]. Section VII concludes the paper and proposes future work.

## II. Related works

Robotic cable manipulation is gaining more attentions recently for its broad applications. In order to accomplish this challenging task, a robust state estimator to track the configuration of the cable in real-time is vital. Metaxas and Terzopoulos [3] constructed a second-order dynamic model for multi-body objects, and recursively estimated the body motion from sequences of point clouds by an extended Kalman filter. Schulman et al. [4] proposed a modified expectation maximization (EM) algorithm for deformable object tracking,

Similarly, Petit et al. [5] introduced a finite element method for tracking elastic objects. Navarro-Alarcon et al. proposed a Fourier-based shape servoing method for deformable object representation [1]. Tang and Tomizuka used a non-rigid registration tracking method called structure preserved registration (SPR) [2]. SPR is able to estimate the positions of virtual tracking points on the deformable object in real-time robustly by considering both the local structure and the global topology of the deformable object (Fig. 2).

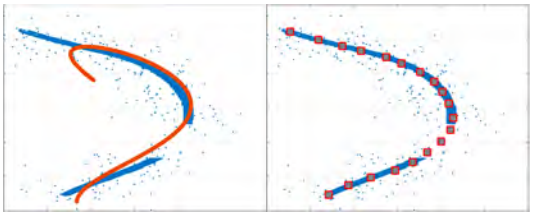

(a) Fourier-Based Estimation (b) SPR Estimation

Fig. 2. Comparison of Fourier-based method and SPR on cable tracking. Blue dots (or the blue line) are the point cloud with outliers and occlusions, and red circles (or the red line) are the estimated position. Fourier-based method fails to estimate the state, while SPR still works well and can give the variance of estimation uncertainty.

For manipulation planning, Morita et al. [8] developed a knot planning from observation (KPO) system which estimated the states of ropes, especially the overlap orders by knot theory. Kudoh et al. [9] built a multi-finger hand and programmed skill motions by imitating human knotting procedures. They realized three dimensional in air knotting with diverse types of knots. However, many of these methods require empirical laws and are developed for a specific task, which is not easy to generalize for other tasks. To generalize the manipulation skills, Schulman et al. [10] proposed to teach robots to manipulate deformable objects from human demonstrations. They implemented the thin plate spline - robust point matching (TPS-RPM) algorithm [11] to warp the original trajectory taught by human demonstration to get a new trajectory which was suitable for the test scene. Tang et al. [7] proposed tangent space mapping method which guaranteed not to overstretch the cable during manipulation. Several follow-up works further improved this demonstration-based method. Tang et al. [12] proposed a uniform framework based on coherent point drift for robustly manipulating deformable linear objects. However, these methods lack the ability to achieve accurate position and can hardly apply to new scenarios which have significant differences with the training scene. Navarro-Alarcon et al. [6] proposed the idea of local deformation model approximation and then utilized the local model to automatically servo-control the soft object to desired shapes. Hu et al. [13] improved the performance by Gaussian process regression. Zhu et al. [14] extended their work by setting up a framework, Fourier-LS, which combines the truncated Fourier series visual servoing method and an efficient continuous local model approximation method. The framework proposed in this paper has a similar structure to the Fourier-LS.

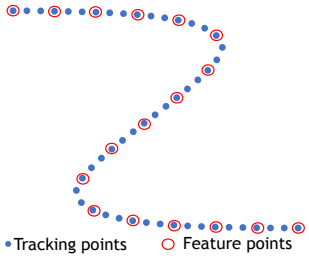


Fig. 3. Illustration of tracking points and feature points.

Compared with other methods, the proposed method SPR-RWLS is the first to take visual tracking uncertainties into consideration for robotic cable manipulation. As shown in Fig. 2, for cable tracking, compared with the Fourier-based visual servoing method, SPR works robustly in the presence of outliers and occlusions. For deformation model approximation, a novel algorithm for solving robust weighted least squares is introduced in this paper. The robust local deformation model for trajectory planning can be obtained efficiently by solving several second-order cone program (SOCP) in parallel. We show that our method is able to obtain robust deformation models in different scenarios with modest computational cost by several experiments.

## III. Structure preserved registration

In order to track the shape of cable, we select finite number of virtual tracking points along the cable to represent the state of the cable. In Fig. 3, the blue dots represent the tracking points, which we select to track the shape of the cable, and the red circles are the feature points, which we use to solve the deformation model in later section. Usually, feature points are a subset of tracking points. Because of the sparsity of feature points, we can assume that the position of every feature point is uncorrelated with other feature points.

### A. Gaussian Mixture Model

We need to estimate the tracking points from the dense and noisy point cloud. Gaussian mixture model (GMM) is

utilized here to estimate the positions of tracking points. In GMM, those tracking points are represented by Gaussian centroids and the point cloud is a set of randomly sampled points from this GMM. We denote the Gaussian centroids as $X^t = [x_1^t, x_2^t, ..., x_N^t] \in \mathbb{R}^{N*D}$, where $x_i^t$ is the position of *i-th* centroid at time step t, $N$ is the number of tracking points and $D$ is the dimension of the position for each tracking point. The point cloud of cable is denoted as $Y^t = [y_1^t, y_2^t, ..., y_M^t] \in \mathbb{R}^{M*D}$, where $y_i^t$ is the position of *i-th* point in the point cloud. $M$ is the total number of points in point cloud and usually $M >> N$. Then the point cloud distribution can be expressed as

$$p(y_m^t) = \sum_{n=1}^{N} \frac{1}{N} \mathcal{N}(y_m^t; x_n^t, \sigma^2 \mathbf{I}) = \sum_{n=1}^{N} \frac{1}{N} \frac{1}{(2\pi\sigma^2)^{D/2}} \exp(-\frac{\|y_m^t - x_n^t\|^2}{2\sigma^2}) \quad (1)$$

All the Gaussians share the same weight. To account for the noise and the outliers of the point cloud, an additional uniform distribution is added to $p(y_m^t)$:

$$p(y_m^t) = \sum_{n=1}^{N+1} p(n) p(y_m^t | n) \quad (2)$$

with

$$p(n) = \begin{cases} (1-\mu)\frac{1}{N}, & n = 1, \ldots, N \\ \mu, & n = N+1 \end{cases} \quad (3)$$

$$p(y_m^t | n) = \begin{cases} \mathcal{N}(y_m^t; x_n^t, \sigma^2 \mathbf{I}), & n = 1, \ldots, N \\ \frac{1}{M}, & n = N+1 \end{cases} \quad (4)$$

where $\mu$ denotes the weight of the uniform distribution.

The Gaussian centroid and corresponding covariance that best represent the point cloud of cable can be obtained by maximizing the following log-likelihood function.

$$L(x_n^t, \sigma^2 | Y^t) = log \prod_{m=1}^{M} p(y_m^t) \quad (5)$$

$$= \sum_{m=1}^{M} log(\sum_{n=1}^{N+1} p(n) p(y_m^t | n)) \quad (6)$$

The above maximization problem is non-convex due to the summation inside $log(.)$ function. Hence, the problem is hard to solve efficiently. Instead of solving the above problem, we aim to maximize the lower bound for (6).

$$Q(x_n^t, \sigma^2) = \sum_{m=1}^{M} \sum_{n=1}^{N+1} p(n | y_m^t) log(p(n) p(y_m^t | n)) \quad (7)$$

It can be proved by Jensen's inequality [15] that (7) is the lower bound of (6). It can be efficiently solved by using EM algorithm in which we iteratively update the GMM parameters and posteriori probability distribution. In the expectation(E) step, we compute the posteriori probability distribution using GMM parameters from the last maximization(M) step. In M step, we compute the new GMM parameters using posteriori probability distribution from the last E step. By iteratively executing E-M step, the log-likelihood function will converge and we can get a pair of local optimal parameters $(x_n^{t*}, \sigma^{2*})$ of GMM.

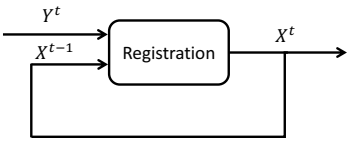


Fig. 4. Framework of point set registration. $Y^t$ is the perceived point cloud at time step t. $X^{t-1}$ is the state estimated at the previous step. A new estimate $X^t$ is achieved by registering $X^{t-1}$ to $Y^t$ .

### *B. Structure Preserved Registration*

Although the above GMM can register the point cloud of the cable to several tracking points, the estimation performance is poor especially when a part of the point cloud is missing, for example when occlusion happens during perception, which is very common in robot manipulation. The major problem is that there are no constraints on the positions of Gaussian centroids between different time steps. In reality, the cable cannot move arbitrarily and its deformation must follow some topological constraints. Globally those registered Gaussian centroids must form a smooth curvature, and locally those Gaussian centroids should maintain certain distance with their neighborhood.

To deal with this problem, we introduce both global and local structure regularization to (7) in GMM registration.

$$\tilde{Q} = Q(x_n^t, \sigma^2) - \frac{\tau}{2} E_{Local} - \frac{\lambda}{2} E_{Global} \quad (8)$$

where $\tau \in \mathbb{R}^+$ and $\lambda \in \mathbb{R}^+$ are trade-off weights that balance the regularization on local and global structure. $E_{Local}$ and $E_{Global}$ are regularization terms which will be explained in the following.

For local structure, any point at time step $t-1$ can be characterized as a weighted sum of its neighbor points. That is $x_n^{t-1} = \sum_{i \in I_n} S_{ni} \cdot x_i^{t-1}$, where $S_{ni}$ is the weight matrix and $I_n$ is the set for $K$ nearest points to $x_n^{t-1}$. When the cable deforms to another shape at time step $t$, the position of tracking points might change, but their relative local structure is expected to be maintained, which means at time step $t$, $x_n^t \approx \sum_{i \in I_n} S_{ni} \cdot x_i^t$. The local structure weights $S_{ni}$ can be obtained by solving a least squares problem. There could be many sub-optimal weights due to the singularity of matrix when solving least squares, so we integrate all $L$ sub-optimal weights to characterize the local structure. More details can be found in [2].

$$E_{Local} = \sum_{n=1}^{N} \sum_{l=1}^{L} || \sum_{i=1}^{N} S_{ni}^{(l)} x_i^t ||^2 \quad (9)$$

Global structure should also be preserved during registration. Since cable in real world cannot move arbitrarily, the registered tracking points should also follow a smooth trajectory in neighboring time step. In order to preserve the global structure, we regularize the coherent movement

$x_n^t = v(x_n^{t-1})$. $v : \mathbb{R}^D \to \mathbb{R}^D$ is a transformation function which should to be as smooth as possible. The smoothness can be evaluated by $\int_{R^D} \frac{|V(s)|^2}{G(s)}$, where $V(s)$ is the Fourier transform of $v$ and $G(s)$ is a low-pass filter.

$$E_{Global} = \int_{R^D} \frac{|V(s)|^2}{G(s)} ds \tag{10}$$

Substituting (9) and (10) into (8) we obtain the modified likelihood function $\tilde{Q}$.

$$\tilde{Q} = Q(x_n^t, \sigma^2) - \frac{\tau}{2} \sum_{n=1}^{N} \sum_{l=1}^{L} || \sum_{i=1}^{N} S_{ni}^{(l)} x_i^t ||^2 - \frac{\lambda}{2} \int_{R^D} \frac{|V(s)|^2}{G(s)} ds \tag{11}$$

Though the global and local structure regularization can be formulated in other different ways, the reason for the above regularization is to obtain closed-form solution for it. This is crucial if we want to solve the problem in real-time. More details about SPR and the proof of the existence of closed-form solution can be found in [2].

## IV. Local Linear Deformation Model

### A. Deformation Model

To approximate the deformation model, we uniformly select several feature points along the cable, which are a subset of the tracking points (Fig. 3).

By holding two tips of the cable, end-effectors of the robots are assumed to be fixed with cable tips. We can build a deformation model for describing the interaction between the end-effectors and the cable. Assuming that there are $N_f$ selected feature points on the cable and the degrees of freedom for each point is $D$. The state of the cable is denoted as $c = [c_1, c_2, ..., c_{N_f}]^T \in \mathbb{R}^{N_f \times D}$, where $c_i = [c_{i1}, c_{i2}, ..., c_{iD}] \in \mathbb{R}^{1 \times D}$, $c_{ij}$ denotes the coordinate of the *i-th* point in the *j-th* direction, for example in 2D space, $c_{5,2}$ denotes the second direction of the 5-*th* selected point. Assume that there are $L$ manipulators and each end-effector has $K$ degrees of freedom. The motion of the robots end-effectors is denoted as $r = [r_{11}, r_{12}, ..., r_{1K}, ..., r_{LK}] \in \mathbb{R}^{L \times K}$. The local linear model we used is expressed in (12) [6]. As shown in (12) the desired local linear model is $\frac{\delta c}{\delta r}$, and each row of $\frac{\delta c}{\delta r}$ is decoupled with each other, therefore we can make use of parallel computation to find linear model $\frac{\delta c_i}{\delta r}$ for each direction simultaneously, which can greatly improve the efficiency.

$$\begin{aligned} \delta c(t) = \begin{bmatrix} \delta c_1(t) \\ \vdots \\ \delta c_{N_f}(t) \end{bmatrix} = \frac{\delta c}{\delta r}(t) \delta r(t) = \begin{bmatrix} \frac{\delta c_1}{\delta r}(t) \\ \vdots \\ \frac{\delta c_{N_f}}{\delta r}(t) \end{bmatrix} \delta r(t) \\ = A(t) \delta r(t) \end{aligned} \tag{12}$$

### B. Local Linear Model

The time-varying deformation model is difficult to obtain due to its high dimensions, nonlinear behaviors and configuration dependent properties. Actually, it is unnecessary to find a global deformation model which is suitable for every possible cable configuration. If the displacement of the robots end-effectors is small enough, the local deformation model can be approximated with linear functions.

The local linear deformation model is expressed in (12), where $A(t) \in \mathbb{R}^{N_f \times LK}$ is a time-varying Jacobian Matrix, which represents the relation between the movement of the robots and the movement of the feature points. Remember that our goal is to plan trajectory for the robots end-effectors to manipulate the deformable cable to a desired shape. To achieve this, we try to find the motion of the robots $\delta r(t)$ given the desired displacement of the cable $\delta c(t)$. For convenience, instead of calculating the Jacobian matrix $A(t)$, we directly find the pseudo-inverse of Jacobian matrix $G(t) = A^{\dagger}(t)$. Since $A(t) \in \mathbb{R}^{N_f \times LK}$, in practice, the number of feature points on the cable is always larger than the DOF of robots end-effectors $N_f >> LK$. Therefore, we can guarantee that $G(t)$ exists.

To estimate $G(t)$, we denote the current time as $t_m$. Using a constant sampling period $\delta t$, within the time period $(m-1)\delta t$, we collect m consecutive data of $\delta c_i$ and $\delta r_i$ while the robot is moving:

$$\begin{aligned} \delta C(t_m) &= \begin{bmatrix} \delta c(t_1) & \delta c(t_2) & . & . & . & \delta c(t_m) \end{bmatrix} \in \mathbb{R}^{N_f \times m} \\ \delta R(t_m) &= \begin{bmatrix} \delta r(t_1) & \delta r(t_2) & . & . & . & \delta r(t_m) \end{bmatrix} \in \mathbb{R}^{LK \times m} \end{aligned}$$

The local linear model can be found by solving (13), which can be decomposed to a sum of several least squares. $G_n^T(t)$ represents the *n-th* column of the matrix $G^T(t)$, and similarly $\delta R_n^T(t)$ represents the *n-th* column of $\delta R_n^T(t)$.

$$\begin{aligned} G(t)^* &= \underset{G(t)}{arg\min} \quad \| \delta C^T(t) G^T(t) - \delta R^T(t) \|_F^2 \\ &= \sum_{n=1}^{LK} \underset{G_n(t)}{arg\min} \quad \| \delta C^T(t) G_n^T(t) - \delta R_n^T(t) \|_2^2 \end{aligned} \tag{13}$$

In the next subsection, we will introduce how to improve the robustness of the local model approximation by using robust optimization.

### C. Robust weighted least squares

The displacement of the robots end-effectors $\delta R(t)$ can be calculated accurately using the robotic forward kinematics. However, $\delta C(t)$ is an estimation with lots of uncertainties from visual tracking. If uncertainties are not considered, we may fail to recover a suitable local deformation model. Uncertainty in $\delta C(t)$ can be approximated by Gaussian distribution, so we are able to bound it inside a certain area given a confidence probability.

In SPR, we regard the tracking points in the last time step as Gaussian centroids and each point in the new point cloud as a sample from the Gaussian mixture model. The objective is to maximize the log-likelihood of the point cloud sampled from the GMM. Thus it is reasonable to regard the variance of each Gaussian as the uncertainty of this movement. Taking the *i-th* point as an example, $\mu(c_i(t))$ is the mean of the *i-th* point at time step $t$, and $\sigma_t$ is the uncertainty from time step $t-1$ to $t$. Besides, we assume

that each Gaussian has an equal membership probability $1/N$ and a consistent isotropic covariance $\sigma^2 I$ in SPR registration. So all the selected tracking points on the cable have the same variance $\sigma_t$ at time step $t$, and all the feature points are uncorrelated.

$$\delta C^T(t) = \mu(\delta C^T(t)) + \Delta \tag{14}$$

(14) shows the uncertainty in the matrix $\delta C^T(t)$ for robust optimization, where $\Delta$ describes the uncertainty. From the above analysis, the $j-th$ column of the matrix $\Delta$ can be regarded as a sample from a Gaussian Distribution $N(0,\Sigma)$, where $\Sigma = diag(\sigma_1^2, \sigma_2^2, ..., \sigma_m^2)$.

We rewrite (13) in the form of robust optimization in (15),

$$\sum_{n=1}^{LK} \min_{G_n(t)} \max_{\|\Delta\|_2 \le s} \quad \|W[(\mu(\delta C^T(t)) + \Delta)G_n^T(t) - \delta R_n^T(t)]\|_2^2 \tag{15}$$

where $s$ is the upper bound or equivalently the largest singular value of $\Delta$, and $W = diag(w_1, w_2, ..., w_m)$ is a weight matrix for the data from different time steps.

When solving the robust optimization problem (15), a tight bound $s$ is preferred. Each column of $\Delta$ can be regarded as a random sample from the Gaussian distribution, and there are some existing works in statistics to bound the largest singular value with a desired probability.

*Theorem 1:* Let $\Delta \in \mathbb{R}^{m\times n}$ be drawn according to the $\Sigma$-Gaussian ensemble. Then for all $\delta > 0$, the maximum singular value $\sigma_{max}(\Delta)$ satisfies the upper deviation inequality,

$$\mathbb{P}[\frac{\sigma_{max}(\Delta)}{\sqrt{n}} \le \gamma_{max}(\sqrt{\Sigma})(1+\delta) + \sqrt{\frac{trace(\Sigma)}{n}}] \ge 1 - e^{-n\delta^2/2}$$

where $\gamma_{max}(\sqrt{\Sigma})$ denotes the largest eigenvalue of $\sqrt{\Sigma}$.

Theorem 1 provides a theoretically tight bound of the random matrix $\Delta$ which is proved in Chapter 6 of [16]. Using this theorem, we can find an upper bound of the largest singular value of uncertainty matrix $\Delta$ given a desired probability.

*Theorem 2:* Any robust least squares in the form:

$$\min_{x\in\mathbb{R}^n} \max_{\|\Delta\|_2 \le s} \quad \|(A+\Delta)x - b\|_2$$

is equivalent to a SOCP problem:

$$\min_{x\in\mathbb{R}^n} \quad \|Ax-b\|_2 + s\|x\|_2$$

*Proof:* For fixed $x$, and using the fact that the Euclidean norm is convex, we have

$$\|(A+\Delta)x - b\|_2 \le \|Ax-b\|_2 + \|\Delta x\|_2$$

By the definition of the largest singular value norm, and given our bound on the size of the uncertainty, we have

$$\|\Delta x\|_2 \le \|\Delta\|_2 \|x\|_2 \le s\|x\|_2$$

Thus, we have a bound on the objective value of the robust least squares problem:

$$\max_{\|\Delta\|_2 \le s} \quad \|(A+\Delta)x - b\|_2 \le \|Ax-b\|_2 + s\|x\|_2$$

The upper bound is actually attained by

$$\Delta = \frac{s}{\|Ax-b\|_2 \|x\|_2}(Ax-b)x^T$$

■

Therefore, the robust weighted least squares (RWLS) in (15) can be written in the form of a summation over several SOCPs as shown in (16). For each SOCP, we find one column of the model matrix $G^T(t)$. The columns of $G^T(t)$ do not depend on each other, which means that we can make use of parallel computation to solve each SOCP and greatly increase the efficiency of the solution process.

$$\sum_{n=1}^{LK} \min_{G_n(t)} \quad \|W\mu(\delta C^T(t))G_n^T(t) - W\delta R_n^T(t)\|_2 + s\|WG_n^T(t)\|_2 \tag{16}$$

If the matrix $G(t)$ is obtained, it means that the local model at time step t is approximated. Given a desired movement of cable, we are able to obtain the trajectory of the robots end-effectors.

## V. Framework Details

### A. Algorithm Overview

Combining the above SPR estimation with RWLS for solving local deformation model, we propose our method 'SPR-RWLS' to manipulate soft cables to desired shapes. SPR is utilized to estimate the cable state in real-time. Robust weighted least squares (RWLS) is used to obtain a robust local deformation model considering tracking uncertainties. The proposed method is summarized in Algorithm 1.

**Algorithm 1:** SPR-RWLS

```
Initialize cable, and record desired cable shape;
Using SPR to get initial and desired tracking points
  along the cable;
Downsample tracking points with a fixed index to get
  feature points;
Initialize data set D(δR, δC) by randomly executing
  robot δR and collecting corresponding movement of
  cable δC for m_0 times;
while diff(c_current, c_desired) > ε do
    Compute weight matrix W;
    Solve Robust Weighted Optimization for local
      deformation Jacobian Matrix G(t);
    Compute δr = λ G(t) δC_desired;
    Execute δr, collect new δc by SPR;
    Append δr and δc to dataset D;
end
```

### B. Cable Tracking

We select $N_{tracking}$ tracking points uniformly distributed along the initial point cloud. At time step $t$, the tracking points are denoted as $X^t = \{x_1^t, x_2^t, ..., x_{N_{tracking}}^t\}$, where $x_n^t \in \mathbb{R}^2$. At the next time step $t+1$, the cable deforms to a new shape, and its point cloud $Y^{t+1} = \{y_1^{t+1}, y_2^{t+1}, ..., y_M^{t+1}\} \in \mathbb{R}^2$ is captured by the camera. By applying SPR registration

as described in Section III, the node positions $X^k$ can be smoothly registered towards the point cloud $Y^{t+1}$, and we can get the new estimation of tracking point positions $X^{t+1}$, and the variance $\sigma_{t+1}$ of this step.

As shown in Fig. 4, running the above procedure iteratively, we can obtain the estimated position of each tracking point in real time.

### C. Deformation Approximation

We select $N_{feature}$ feature points from the tracking points just as Fig. 3 shows. Also at time step $t$, the movement of each feature point $\delta c(t) = c(t) - c(t-1)$, and the tracking uncertainties of this step $\sigma_k$ can be obtained from SPR registration. The movement of the robots end-effectors $\delta r$ can also be calculated by forward kinematics. Then we append these new data $\delta c(t)$, $\delta r(t)$, and $\sigma_t$ to data set $\delta C(t)$, $\delta R(t)$, and $\Sigma(t)$ respectively. Before we calculate the deformation model, we assign weights to different $(\delta r, \delta c)$ pairs in the data set. We rank the data pairs in data set based on their mean squared errors to the current cable shape. A discount factor $\gamma$ is used to assign weights to different data pairs. The discount factor is a tuning parameter and we use 0.95 in our experiments. Besides, the bound of the uncertainties can be efficiently calculated by a given confidence probability. In practice, we set the confidence probability larger than 99%. Finally, the local deformation model $G(t)$ can be solved by the robust optimization problem (16).

By running this algorithm iteratively, we are able to get an approximation of the deformation model in real-time.

### D. Trajectory Planning

After the deformation model $G(t)$ is obtained at time step $t$, we first need to compute the desired movement of the cable $\delta c_{desired}(t)$ in order to get the motion of the robots. For the scenarios which desired shape is far away from the initial shape, several intermediate desired shapes $c_{intermediate}$ are preferred to be generated and reached in sequence. In order to achieve such $\delta C$, the desired movement of end-effectors is computed using $\delta r(t) = \lambda G(t) \delta c_{desired}(t)$, where $\lambda$ is a gain we need to tune. In order to make the cable moving in a low speed without vibration and make sure the deformation model is locally accurate, the gain $\lambda$ is chosen to be small. In our experiment, $\lambda$ is set to 0.1.

## VI. Experiments and Results

We conduct several experiments on two FANUC LR-Mate 200iD robots to show that SPR-RWLS is efficient and robust in the presence of outliers and occlusions for robotic cable manipulation.

### A. Cable Tracking

As shown in Fig.5, an IDS Ensenso N35 stereo camera was utilized to monitor the environment. The captured point cloud was sent to a Windows 10 desktop (Intel i7@3.60 GHz + RAM 8GB), which ran SPR registration algorithms in real-time in MATLAB. Using a color filter, the point cloud of the cable was extracted from the red background. Since the cable was manipulated in a two dimensional plane, $3D$ point cloud was projected to the $2D$ plane. Given the initial point cloud of a straight cable, we manually selected 55 tracking points uniformly distributed along the cable. When the cable deformed to a different shape in the next step, we registered the newest point cloud to the point cloud from the last time step using SPR. Then the corresponding 55 tracking points which represent the current cable state were obtained.

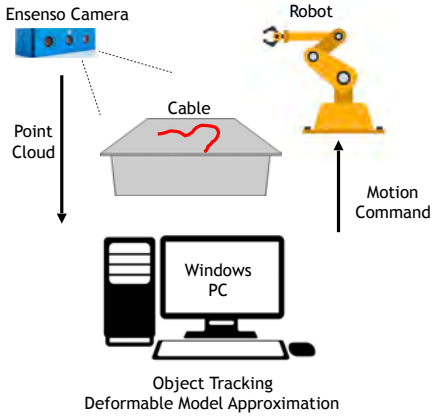


Fig. 5. The testbed setup

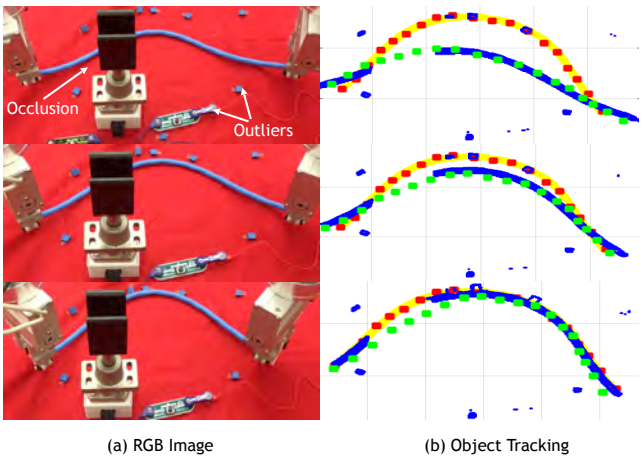


Fig. 6. SPR cable tracking in the presence outliers and occlusions. In (b), blue dots represent the perceived point cloud; yellow dots represent the target shape; red squares represent the desired feature points; and green squares represent current feature points.

Tracking results show that SPR cable tracking module is able to robustly track the movement of the cable in real-time. SPR outperforms Fourier-Based estimation when the point cloud is contaminated by outliers, noise, and occlusions. When manually adding white noise to the point cloud and removing 20% of the point cloud from the middle part to simulate occlusions (Fig. 2), Fourier-Based estimation fails tracking the cable, while SPR is still able to provide a robust estimation of the cable position as well as estimation of the uncertainties. Fig.6 shows SPR tracking performance in the presence of occlusions and outliers due to objects of similar

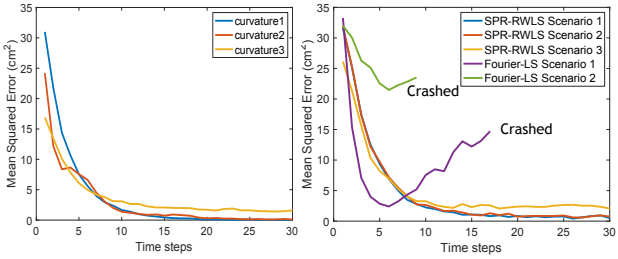


(a) SPR-RWLS performance

(b) Comparison of Fourier-LS and SPR-RWLS under outliers and occlusions

Fig. 7. Mean Squared Error vs Timesteps. (a) shows the results of manipulation a cable to different curvatures, which are shown in Fig. 8, and (b) compares SPR-RWLS with Fourier-LS in different scenarios, which are introduced in Section VI.B

TABLE I

EXPERIMENTS WITH DIFFERENT CABLES

| Cable diameters | Success rate | Mean squared error ($cm^2$) |
|---|---|---|
| $4.04mm$ | 9/10 | $0.242 \pm 0.079$ |
| $8.10mm$ | 10/10 | $0.051 \pm 0.014$ |

TABLE II

COMPARISON OF MEAN SQUARED ERROR OF OUR ROBUST METHOD AND FOURIER-LS METHOD

| Feature | Fouriers-LS | SPR-RWLS |
|---|---|---|
| No outliers and occlusions | $0.045 \pm 0.026 cm^2$ | $0.051 \pm 0.014 cm^2$ |
| Uncertainty scenario 1 | $14.712 \pm 1.5832 cm^2$ | $0.411 \pm 0.093 cm^2$ |
| Uncertainty scenario 2 | $23.45 \pm 1.259 cm^2$ | $0.629 \pm 0.1623 cm^2$ |
| Uncertainty scenario 3 | fail | $2.503 \pm 0.438 cm^2$ |

colors to the cable appear in the work space.

### B. Cable Manipulation

To evaluate the performance of the proposed framework, we conducted experiments to manipulate cables of different thickness under different scenarios. The goal is to manipulate the cable from straight lines to given desired shapes. Experimental videos can be found in [17].

The robots end-effectors are parallel grippers which can open and close. When closing, the gripper can clamp the cable firmly without any slipping. Since the experiment is conducted on a $2D$ plane, each end-effector has 3 degrees of freedom including two orthogonal displacement on horizontal plane and one rotation along axis that is perpendicular to the horizontal plane. For the model approximation, ECOS [18], an efficient SOCP solver, was utilized to solve the problem (16).

Given the positions and variances of 55 estimated tracking points from SPR, we select 19 feature points from the tracking points to estimate the deformation model. Each feature point has two degrees of freedom in $2D$ plane. Using Algorithm 1 introduced in section V, several experiments are conducted to test the proposed framework. We use the mean squared distance errors of 55 tracking points between the cable and the desired shape to evaluate the manipulation performance.

A sequence of snapshots is shown in Fig.8. The cable was successfully manipulated from a straight line to given desired curvatures. For a simple desired shapes (Fig.8 (a), (b)), the manipulated cable overlaps with the desired shape perfectly with the mean squared error (MSE) smaller than 0.08 $cm^2$. For complicated desired shapes with more curvatures (Fig.8 (c)), the MSE is about 1.5 $cm^2$. Fig. 7 (a) shows that the MSE converges over time steps.

The performance of the algorithm with different cables is analyzed in Table I. We conducted experiments with two cables of different diameters. One Ethernet cable has a diameter of $4.04mm$, and the other cable has a diameter of $8.10mm$. We manipulate both cables to the same simple desired shape (curvature 1 in Fig.8) 10 times. Both experiments have very high success rates. The thinner cable has a little bit higher MSE. It is reasonable because the thinner cable is more likely to deform, which makes the deformation model not accurate.

We also performed several experiments to show that SPR-RWLS is able to perform robustly in the presence of outliers and occlusions. As shown in Table II, we conducted experiments to manipulate the blue Ethernet cable to curvature 1 in 4 different scenarios. In the first scenario where there are no outliers and occlusions, both Fourier-LS and SPR-RWLS performe very well. Uncertainty scenario 1,2 and 3 are the scenarios in the presence of noise, outliers, and occlusions. In uncertainty scenario 1, we manually occluded 20% of the point cloud, and added 5% white noise with $\sigma = 10\%\delta c$. In uncertainty scenario 2, we occluded 25% point cloud, and added 10% white noise with $\sigma = 15\%\delta c$. Uncertainty scenario 3 is shown in Fig.6, where objects of color similar to the Ethernet cable are placed on the table and part of the Ethernet is occluded by other objects. In Table II, we can clearly see that SPR-RWLS outperforms Fourier-LS [14] in the presence of noise, outliers, and occlusions.

## VII. CONCLUSION AND FUTURE WORK

In this paper, a novel framework SPR-RWLS for cable manipulation is proposed. In the framework, we combine real-time cable tracking and online deformation model approximation. For real-time tracking, a Gaussian mixture model based non-rigid registration is able to track deformable cable robustly in the presence of sensor noise, outliers, and occlusions. For deformation model approximation, the local deformation model can be approximated online by solving a robust optimization in parallel under uncertainty. Experiments showed that the proposed method is able to manipulate deformable cable to desired shape robustly.

For future work, we plan to test the performance on more complicated desired shapes. For a desired shape that is far from the initial shape or when the cable is too long, we plan to develop a method that can automatically and efficiently generate intermediate desired shapes. SPR is proved to be robust for deformable cable tracking in $3D$ space. More manipulation tasks with deformable cable and deformable $2D$ cloth will be tested in $3D$ space.

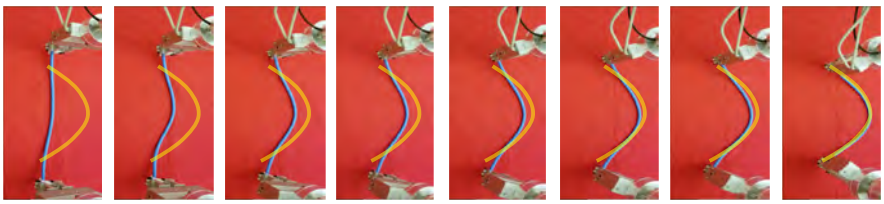

(a) Curvature 1

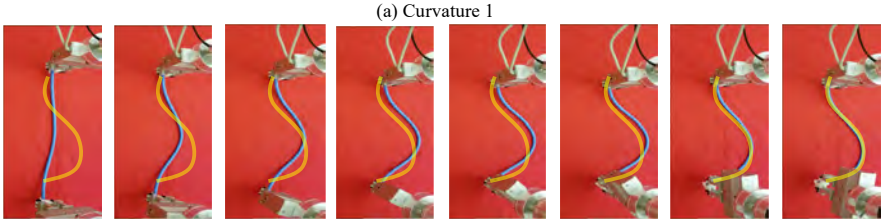

(b) Curvature 2

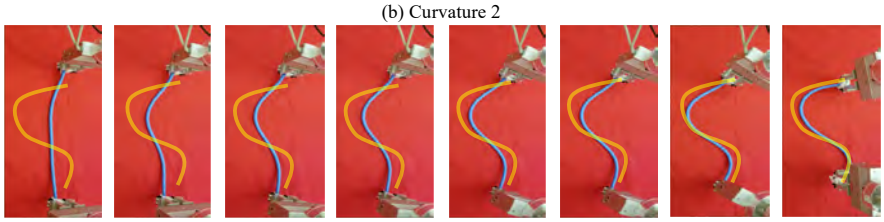

(c) Curvature 3

Fig. 8. Snapshots of the cable manipulation experiments. Two robot arms were collaborating to manipulate a cable to desired shapes, which are shown by the yellow lines. (a), (b), and (c) show three different curvatures.

## REFERENCES


[1] D. Navarro-Alarcon and Y. H. Liu, Fourier-based shape servoing: A new feedback method to actively deform soft objects into desired 2-d image contours, T-RO, vol. 34, no. 1, pp. 272-279, Feb 2018.

[2] T. Tang and M. Tomizuka, Track deformable objects from point clouds with Structure Preserved Registration, Int. J. Robot. Res., 2019, in press.

[3] D. Metaxas and D. Terzopoulos, Shape and nonrigid motion estimation through physics-based synthesis, IEEE Transactions on Pattern Analysis and Machine Intelligence 15(6): 580-591, 1993

[4] J. Schulman, A. Lee, J. Ho and P. Abbeel, Tracking deformable objects with point clouds, In: Robotics and Automation (ICRA), IEEE International Conference on. IEEE, pp. 1130-1137, 2013

[5] A. Petit, V. Lippiello and B. Siciliano, Real-time tracking of 3d elastic objects with an rgb-d sensor, In: Intelligent Robots and Systems (IROS), 2015 IEEE/RSJ International Conference on. IEEE, pp. 3914-3921, 2015

[6] D. Navarro-Alarcon, Y. H. Liu, J. G. Romero and P. Li, Model-Free visually servoed deformation control of elastic objects by robot manipulators, IEEE Trans. Robot., 26(6):1457-1468, 2013.

[7] T. Tang, C. Liu, W. Chen and M. Tomizuka, Robotic manipulation of deformable objects by tangent space mapping and non-rigid registration, International Conference on Intelligent Robots and Systems (IROS), 2016.

[8] T. Morita, J. Takamatsu, K. Ogawara, H. Kimura, and K. Ikeuchi, Knot planning from observation, in Proc. IEEE Int. Conf. Robot. Autom., vol. 3, pp. 3887-3892, 2003.

[9] S. Kudoh, T. Gomi, R. Katano, T. Tomizawa, and T. Suehiro, In-air knotting of rope by a dual-arm multi-finger robot, in Proc. IEEE/RSJ Int. Conf. Intell. Robots Syst., pp. 6202-6207, 2015.

[10] J. Schulman, J. Ho, C. Lee, and P. Abbeel, Learning from demonstrations through the use of non-rigid registration, in Proc. 16th Int. Symp. Robot. Res., Springer, Cham, pp. 339-354, 2016.

[11] H. Chui and A. Rangarajan, A new point matching algorithm for nonrigid registration, Comput. Vis. Image Understanding, vol. 89, no. 2, pp. 114-141, 2003.

[12] T. Tang, C. Wang, and M. Tomizuka, A framework for manipulating deformable linear objects by coherent point drift, IEEE Robotics and Automation Letters, vol. 3, no. 4, pp. 3426-3433, 2018.

[13] Z. Hu, P. Sun, and J. Pan, Three-dimensional deformable object manipulation using fast online gaussian process regression, IEEE Robotics and Automation Letters, vol. 3, no. 2, pp. 979-986, 2018.

[14] J. Zhu, B. Navarro, P. Fraisse, A. Crosnier and A. Cherubini, Dual-arm robotic manipulation of flexible cables, International Conference on Intelligent Robots and Systems (IROS), 2018.

[15] M. Kuczma, An introduction to the theory of functional equations and inequalities: Cauchys equation and Jensens inequality, Springer Science Business Media, 2009.

[16] M. Wainwright, High-dimensional statistics: A non-asymptotic viewpoint, Cambridge University Press, 2019.

[17] Supplementary Videos for SPR-RWLS Cable Manipulation https://changhaowang.github.io/IROS2019/SPRRWLS.html

[18] A. Domahidi, E. Chu, and S. Boyd, ECOS: An SOCP solver for embedded systems, 2013 European Control Conference (ECC) pp. 3071-3076, 2013.